Molecular Precursors in the Dissociative Adsorption of O_2 on Pt(111)

A. Eichler and J. Hafner

Institut für Theoretische Physik and Center for Computational Materials Science, Technische Universität Wien, Wiedner Hauptstraße 8-10/136, A-1040 Wien, Austria

(Received 16 July 1997)

Ab initio local-spin-density calculations for the adsorption of O_2 on Pt(111) are presented. We identify two distinct, but energetically almost degenerate chemisorbed precursors. A superoxolike paramagnetic precursor is formed at the bridge site, with the molecule parallel to the surface. A second peroxolike nonmagnetic precursor is formed in the threefold hollow, with the atom slightly canted in a top-hollow-bridge geometry. The nature of the barrier for dissociation into atoms adsorbed in the hollows is explored. [S0031-9007(97)04669-3]

PACS numbers: 82.65.My, 34.50.Dy, 73.20.At

Trapping into a physisorbed state, chemisorption in molecular form and dissociation are considered to be the fundamental steps in gas-surface interactions [1]. However, despite the experimental evidence for the existence of physisorbed (van der Waals bonded) and chemisorbed molecular precursors to dissociation there are still many open questions concerning the geometric, electronic, and magnetic properties of molecules in the precursor states. In principle, the dissociative adsorption of a diatomic molecule on a rigid surface can be described in terms of a six-dimensional potential-energy surface (PES). Precursor states can be identified in terms of local minima on the PES. Because of the recent progress in *ab initio* total-energy calculations using density-functional techniques, a determination of a six-dimensional PES from first principles is now within reach. However, so far such calculations have been performed only for the most simple cases such as H_2 on Pd(100) [2] or Rh(100) [3] where dissociation occurs in a direct process via activated and nonactivated pathways. The intention of the present work is to perform an *ab initio* density-functional study of the formation of chemisorbed molecular precursors.

The system selected for our study is O_2/Pt(111), both because of the importance of Pt as a catalyst in oxidation reactions and because the different adsorption phases have been thoroughly investigated using various spectroscopic techniques. Photoemission spectroscopy of valence states [4,5] and core levels [6,7], electron energy loss spectroscopy (EELS) [5,8], thermal desorption spectroscopy (TDS) [4,8,9], and near-edge x-ray absorption spectroscopy (NEXAFS) [10–12] have distinguished a physisorbed state and molecular as well as atomic chemisorbed phases. While there is general agreement that during the chemisorption process charge transfer from the substrate to the molecular $1\pi_g$ orbital of the adsorbate leads to a profound modification of the molecular bond, there is disagreement on the precise nature of the chemisorbed molecular state: While the EELS results have first been interpreted in terms of a nonmagnetic peroxolike O_2^{2-} phase, a paramagnetic superoxolike O_2^- state has been postulated on the basis of the NEXAFS data [11]. EELS studies [5,8] have also revealed the existence of two different O-O stretching frequencies, and the possible coexistence of two different chemisorbed molecular species is also supported by different core-level spectroscopies [7]. The two different chemisorbed states have been interpreted as due to adsorption at steps or due to two different adsorption sites. A common conclusion of all these studies is that dissociation of O_2 on Pt(111) is a thermally activated process that occurs at $T > 150$ K via a molecular precursor (or molecular precursors) and that atomic oxygen is adsorbed in the threefold hollows.

Our investigations have been performed in two steps: In the first we explore in detail the potential-energy surface of the O_2 molecule in contact with the Pt(111) surface, and we identify two metastable minima representing two distinct molecular precursor states. In the second step we analyze in detail the electronic and magnetic properties of the precursor states.

The calculations have been performed using a spin-polarized version of the Vienna *ab initio* simulation program VASP [13,14]. VASP performs an iterative solution of the generalized Kohn-Sham equations of local-spin density (LSD) theory via an unconstrained minimization of the norm of the residual vector to each eigenstate and optimized routines for charge- and spin-density mixing. Exchange and correlation are described by the functional proposed by Perdew and Zunger [15], adding nonlocal corrections in the form of the generalized-gradient approximation (GGA) of Perdew *et al.* [16]. The calculations are performed in a plane-wave basis, using fully nonlocal Vanderbilt-type ultrasoft pseudopotentials to describe the electron-ion interaction [17]. The Pt(111) substrate is modeled by a four-layer slab with a rectangular $\sqrt{3} \times 2$ unit cell [leading to a $c(4 \times 2)$ structure], separated by a 14 Å thick vacuum layer. Tests with an eight-layer slab have shown that even for the final adsorption configuration in the fcc hollow (where the adsorbate sinks deepest into the substrate), the adsorption energy changes only by 23 meV. Oxygen is adsorbed on

both sides of the slab, at one molecule per cell the atomic coverage is $\Theta = 0.5$. Brillouin-zone integrations have been performed on a grid of $3 \times 4 \times 1$ $\vec{k}$ points, using a Methfessel-Paxton smearing [18] of $\sigma = 0.2$ eV. All calculations have been performed at the equilibrium lattice constant of $a = 3.99$ Å (experimental $a = 3.92$ Å). Most calculations have been performed at a fixed substrate geometry, but for the molecular precursors a full relaxation of the adsorbate/substrate complex has been allowed.

The potential-energy surface was explored by calculating the potential energy as a function of the distance z from the surface and the bond length d of the O_2 molecule along various reaction channels. Figure 1 shows the surface cell and defines a shorthand notation for special points in the surface cell (t—on top; b—bridge; fcc, hcp—threefold hollows, nt—"near top") and for the reaction channels covered in our study. Channels 1 to 5, together with the channels 2′ to 4′ located around the hcp instead of the fcc hollow explore the variation of the potential energy (PE) as a function of the coordinates x, y in the surface cell. The dependence of the PE on the angle φ for "helicopter" rotations parallel to the surface is tested in channels 5 and 7 for rotations around the top sites, in channels 2 and 6 (2′ and 6′) around the fcc (hcp) hollows, and in channels 1, 8, 9, 10 for rotations about the bridge sites. Because of symmetry in all these fourteen reaction channels except channels 6, 6′ the PE is stationary with respect to the angle Θ for "cartwheel" rotations. Close to the local minimum of the PE we have relaxed all six degrees of freedom of the O_2 molecule. Figure 2 displays the variation of the PE at the bottom for all fourteen channels as a function of the reaction coordinate s measuring the distance from the starting point along the path of minimum PE, beginning at a distance of 4 Å from the surface (at this point we set $s = z = 4$ Å, s decreases when we approach the surface). Along channels 3 to 5, 3′ to 4′, 7, 8, and 10 the dissociative adsorption of O_2 is a direct, strongly activated process with barriers varying between ~0.3 and ~1.5 eV. The adsorption energy is largest in the fcc hollows ($E_{ad} = -1.65$ eV/molecule) and considerably smaller in the hcp hollows ($E_{ad} = -0.99$ eV/molecule).

Along channels 1, 2, 6, 2′, 6′ we observe various local minima that can be identified with molecular precursors. In channel 1 we find a very deep PE minimum of $E_{ad} = -0.72$ eV/molecule at a distance of $z = 1.92$ Å, corresponding to a bond length stretched to $d = 1.39$ Å. Comparison of channel 1 with the neighboring channels 2, 2′ (shifted along the y axis) and 10, 8, 9 (corresponding to helicopter rotations over the bridge position) demonstrates that translation as well as rotation lead to a rapid increase of the PE, so that this configuration corresponds to a molecule chemisorbed parallel to the surface in a t-b-t position. Other local minima are identified in channels 6 and 6′ [b-fcc(hcp)-t]. The energies are -0.18 to -0.27 eV/molecule for a position of the molecule parallel to the surface, at a height of $z \simeq 1.84$ Å. For configurations 6 and 6′ the PE is not stationary with respect to cartwheel rotations. A free minimization of the PE starting from these configurations leads to the two essentially equivalent molecular precursor states described in Fig. 3: an O_2 molecule stretched to $d = 1.43(1.42)$ Å is adsorbed close to the fcc (hcp) hollow, in a position oriented from top to bridge and slightly canted with respect to the surface plane. The adsorption energy is $E_{ad} = -0.68(-0.58)$ eV/molecule, compared to the configuration parallel to the surface the molecule sinks somewhat deeper into the hollow, $z = 1.78(1.81)$ Å. Experimentally, the adsorption energy in the precursors

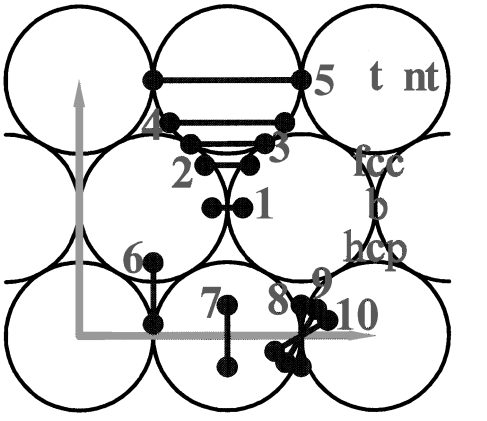

FIG. 1. Surface cell and geometry of the reaction channels explored in our study, together with a shorthand notation for special points. Cf. text.

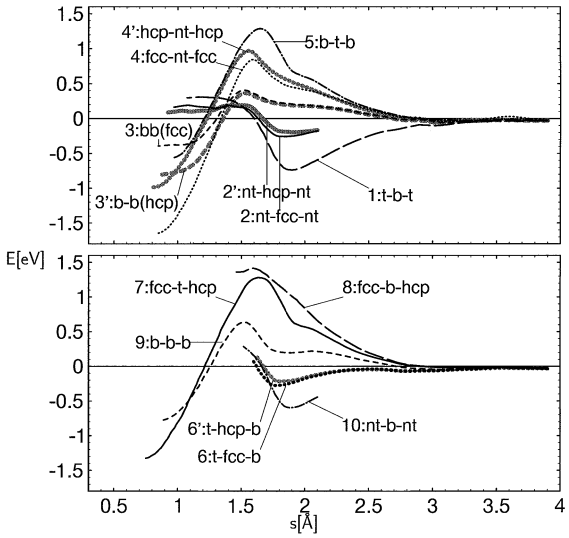

FIG. 2. Variation of the potential energy along the bottom of the fourteen reaction channels defined in Fig. 1 and in the text. The reaction coordinate s measures the distance from the starting point 4 Å above the surface plane along the deepest points in each channel (cf. text).

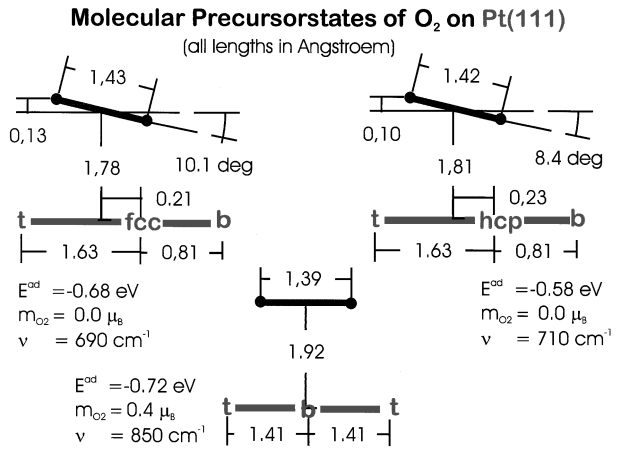

FIG. 3. Geometrical characterization of the chemisorbed molecular precursor states given in addition the adsorption energy E_{ad}, the magnetic moment m_{O_2}, and the stretching frequency ν of the adsorbed molecule.

have been estimated as -0.4 eV/molecule (Ref. [19]) and -0.5 eV/molecule (Ref. [5]). The difference is to be attributed to the one-dimensional model used to analyze the experimental data, and to the notorious overbinding tendency of the LSD theory, which is not completely cured by the GGA.

Hence our calculations support the conjecture [5,8,7] of the existence of two distinct but energetically almost degenerate chemisorbed molecular precursor states for O_2 on Pt(111). In the first state, the molecule is adsorbed in a symmetric t-b-t position characterized by a bond length of $d = 1.39$ Å and an O-O stretching frequency of $\nu = 850\ \mathrm{cm}^{-1}$. The predicted bond length is in good agreement with the experimental estimates based on NEXAFS ($d = 1.37$ Å, Ref. [12]) and photoemission spectroscopy ($d = 1.39$ Å, Ref. [7]), the stretching frequency is confirmed by various EELS measurements ($\nu = 842\ \mathrm{cm}^{-1}$, Ref. [8], $\nu = 875\ \mathrm{cm}^{-1}$, Ref. [5], $\nu = 870\ \mathrm{cm}^{-1}$, Ref. [19]). In the second state, the molecule sits in a slightly asymmetric t-fcc(hcp)-b position in a threefold hollow, with a bond length of $d = 1.43(1.42)$ Å and a stretching frequency of $\nu = 690(710)\ \mathrm{cm}^{-1}$. Again this is in good agreement with estimates based on photoemission spectroscopy ($d = 1.40$ Å, Ref. [20]; $d = 1.43$ Å from core-level and $d = 1.47$ Å from valence-band spectra, Ref. [7]) and EELS ($\nu = 700\ \mathrm{cm}^{-1}$, Ref. [5,8]; $\nu = 710\ \mathrm{cm}^{-1}$, Ref. [19]. Note that the adsorption sites determined for the two precursor species differ to some extent from those proposed previously in the literature [5,7], but agree rather well with a recent scanning tunneling microscopy (STM) study published while this manuscript was being completed [21] (although a detailed calculation of the STM intensities remains to be done).

A complete relaxation of the adsorbate/substrate complex close to the molecular precursors does not change this picture: The relaxation leads to a slight increase of the adsorption energies (by 130 meV for the t-b-t, and by 80 meV for the t-fcc-b precursor), but does not affect their relative stability, bond length, or adsorption height. The t-b-t precursor drifts 0.04 Å away from the b position into the direction of the fcc hollow; there is a slight buckling of the surface (Pt rows carrying O_2 move outwards by 0.09 Å, the intermediate rows inwards by 0.08 Å). Atoms around the t-fcc-b precursor move only slightly such as to increase the size of the hollow.

Our calculations also allow for a unique characterization of the electronic and magnetic properties of the molecular precursors. Figures 4(a) and 4(c) show the isosurfaces of the difference electron densities and the spin density of the precursor in the t-b-t configuration. We find that the charge flow from the substrate to the adsorbate tends to fill the $\pi_{\perp}^{\star}$ antibonding states oriented perpendicular to the surface. The filling of the $\pi_{\perp}^{\star}$ states, but not the $\pi_{\parallel}^{\star}$ states is also corroborated by the analysis of the spin densities [Fig. 4(c)] which show that the remaining magnetic moment of $m_{\mathrm{O}_2} = 0.4\ \mu_B$ is carried by the $\pi_{\parallel}^{\star}$ states only—in contrast to the free O_2 molecule where the spin density is distributed homogeneously over both types of π states [see Fig. 4(d)]. Note that there is an induced magnetization of d_{xz} symmetry of the Pt atoms interacting with the adsorbate. The precursor in the t-fcc-b configuration, on the other hand, has no magnetic moment; the difference electron densities demonstrate an increased occupation of $\pi_{\perp}^{\star}$ and $\pi_{\parallel}^{\star}$ states [see Fig. 4(b)], which is also confirmed by a detailed analysis of the local partial densities of states (results will be published elsewhere). Again our charge-density analysis agrees with the results of the scanning tunneling microscopy studies [21]

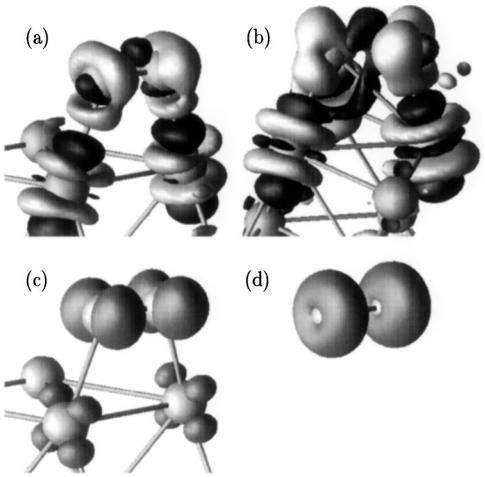

FIG. 4. (a), (b) Isosurfaces of the difference electron densities $[\rho(\mathrm{Pt}(111) + \mathrm{O}_2) - \rho(\mathrm{Pt}(111)) - \rho(\mathrm{O}_2)]$ for (a) the superoxo precursor in the t-b-t configuration and (b) the peroxo precursor in the t-fcc-b configuration. Charge flows from the dark into the light regions. (c), (d) Isosurfaces of the spin densities in (c) the superoxo precursor and (d) the free O_2 molecule.

interpreted in terms of a symmetric $\pi_{\parallel}^{\star}$ state for the t-b-t and a slightly asymmetric "pear-shaped" charge-density distribution with the brighter feature on the top site for the t-fcc-b-precursor. Hence the results for the bond lengths, the stretching frequencies, and the charge and spin densities support an interpretation of the t-b-t precursor as a paramagnetic O_2^- "superoxo" state and of the t-fcc(hcp)-b precursors as a nonmagnetic O_2^{2-} "peroxo" state (the exact quantification of the charge state depending on the details of the local projections of the valence states). Very recently the coexistence of O_2^- and O_2^{2-} states has been predicted by Gravil *et al.* [22] for O_2 on Ag(110). However, because of the differences in the adsorption energies and heights, the O_2^- state was attributed to physisorption and only the O_2^{2-} state to chemisorption.

The energetically most favorable locations for the dissociated atoms are the threefold fcc hollows (cf. Fig. 2), whereas the hcp hollows are much less favorable. This indicates a substantial interaction of the adsorbate with the first subsurface layer. The characteristic stretching frequency for the atomic adsorbate is $\nu = 470\ \mathrm{cm}^{-1}$, to be compared with experimental values of $\nu = 471\ \mathrm{cm}^{-1}$, Ref. [19]; $\nu = 480\ \mathrm{cm}^{-1}$, Ref. [5]).

Both precursors are separated by a substantial barrier from the dissociated chemisorbed atomic state. Realistic scenarios for overcoming the barrier are t-b-t to nt-hcp-nt to fcc-nt-fcc (i.e., a parallel shift of the atom in the y direction, cf. Fig. 2) or t-hcp-b to nt-hcp-nt to fcc-nt-fcc (i.e., a rotation about the hollow followed by a shift sideways). In both cases we find (assuming a rigid surface) a barrier of about 0.18 eV/molecule relative to the free O_2 molecule, corresponding to barriers of 0.86 and 0.90 eV/molecule relative to the precursor states. It must be left to a more detailed exploration of the transition state (including the effect of substrate relaxation and of a lower symmetry of the reaction path) whether the dissociation barrier can be reduced to a value comparable to the desorption barrier, as proposed by Luntz *et al.* [9].

In summary, at distances of 1.8 to 1.9 Å above the surface we find two distinct molecular precursors: one is in a paramagnetic superoxo state, it is formed at the bridge site in a flat top-bridge-top geometry. The second precursor is in a nonmagnetic peroxo state and located at the hollow site in a slightly canted top-hollow-bridge configuration. Geometry and charge densities are in good agreement with STM studies. The calculated stretching frequencies for both precursors agree with EELS experiments; the fact that the precursors are energetically almost degenerate is confirmed by the interpretation of the desorption explored. A certain discrepancy exists for the relative heights of the dissociation and desorption barriers—this will require a more detailed dynamical exploration of the transition state allowing for an eventual phonon-assisted lowering of the barrier.

This work has been supported by the Austrian Science Funds (Fonds zur Förderung der wissenschaftlichen Forschung in Österreich) under Project No. FWF P11353-PHYS.

[1] G. Somorjai, *Introduction to Surface Chemistry and Catalysis* (Wiley, New York, 1994).
[2] A. Gross, S. Wilke, and M. Scheffler, Phys. Rev. Lett. **75**, 2718 (1995); S. Wilke and M. Scheffler, Phys. Rev. B **53**, 4926 (1996).
[3] A. Eichler, G. Kresse, and J. Hafner, Phys. Rev. Lett. **77**, 1119 (1996).
[4] J. Grimblot, A. C. Luntz, and D. E. Fowler, J. Electron Spectrosc. Relat. Phenom. **52**, 161 (1990).
[5] H. Steininger, S. Lehwald, and H. Ihbach, Surf. Sci. **17**, 342 (1982).
[6] W. Ranke and H. J. Kuhr, Phys. Rev. B **39**, 1595 (1989).
[7] C. Puglia, A. Nilsson, B. Hernnäs, O. Karis, P. Bennich, and N. Martensson, Surf. Sci. **342**, 119 (1995).
[8] N. R. Avery, Chem. Phys. Lett. **96**, 371 (1983).
[9] A. C. Luntz, M. D. Williams, and D. S. Bethune, J. Chem. Phys. **89**, 4381 (1988); A. C. Luntz, J. Grimblot, and E. E. Fowler, Phys. Rev. B **39**, 12 903 (1989).
[10] J. Stöhr, J. L. Gland, W. Eberhardt, D. Outka, R. J. Madix, F. Sette, R. J. Koestner, and U. Doebler, Phys. Rev. Lett. **51**, 2414 (1983).
[11] D. A. Outka, J. Stöhr, W. Jark, P. Stevens, J. Solomon, and R. J. Madix, Phys. Rev. B **35**, 4119 (1987).
[12] W. Wurth, J. Stöhr, P. Feulner, X. Pan, K. R. Bauchspiess, Y. Baba, E. Hudel, G. Rocker, and D. Menzel, Phys. Rev. Lett. **65**, 2426 (1990).
[13] G. Kresse and J. Hafner, Phys. Rev. B **47**, 558 (1993); **49**, 14 251 (1994).
[14] G. Kresse and J. Furthmüller, Phys. Rev. B **54**, 11 169 (1996); Comput. Mater. Sci. **6**, 15 (1996).
[15] J. P. Perdew and A. Zunger, Phys. Rev. B **23**, 5048 (1981).
[16] J. P. Perdew, J. A. Chevary, S. H. Vosko, K. A. Jackson, M. R. Pedersen, D. J. Singh, and C. Frolhais, Phys. Rev. B **46**, 6671 (1992).
[17] D. Vanderbilt, Phys. Rev. B **41**, 7892 (1990); G. Kresse and J. Hafner, J. Phys. Condens. Matter **6**, 8245 (1996).
[18] M. Methfessel and A. Paxton, Phys. Rev. B **40**, 3616 (1989).
[19] J. L. Gland, B. A. Sexton, and G. B. Fisher, Surf. Sci. **95**, 587 (1980).
[20] W. Eberhardt, T. Upton, S. Cramm, and L. Incoccia, Chem. Phys. Lett. **146**, 561 (1988).
[21] B. C. Stipe, M. A. Rezaei, W. Ho, S. Gao, M. Persson, and B. I. Lundqvist, Phys. Rev. Lett. **78**, 4410 (1997).
[22] P. A. Gravil, D. M. Bird, and J. M. White, Phys. Rev. Lett. **77**, 3933 (1996).